

JET-P(87)38

D.F. Düchs

# Creation of Electric Fields in Tokamak Plasmas

# Creation of Electric Fields in Tokamak Plasmas

D.F. Düchs

*JET-Joint Undertaking, Culham Science Centre, OX14 3DB, Abingdon, UK*

Preprint of Paper to be submitted for publication in  
Nature Journals

“This document contains JET information in a form not yet suitable for publication. The report has been prepared primarily for discussion and information within the JET Project and the Associations. It must not be quoted in publications or in Abstract Journals. External distribution requires approval from the Publications Officer, JET Joint Undertaking, Abingdon, Oxon, OX14 3EA, UK”.

“Enquiries about Copyright and reproduction should be addressed to the Publications Officer, EFDA, Culham Science Centre, Abingdon, Oxon, OX14 3DB, UK.”

The contents of this preprint and all other JET EFDA Preprints and Conference Papers are available to view online free at [www.iop.org/Jet](http://www.iop.org/Jet). This site has full search facilities and e-mail alert options. The diagrams contained within the PDFs on this site are hyperlinked from the year 1996 onwards.



## 1. Introduction

Electric fields are usually not considered explicitly in tokamaks except for those induced by external coil currents. However, a number of asymmetries, anomalous flows and transport, could be, at least formally, attributed to the action of an  $\vec{E}$ -field. In this paper several mechanisms for electric field creation are pointed out on the basis of illustrative classical physics mechanisms. The pictures are developed for the example of neutral beam injection in Sections 2 to 8, and then transferred to a recycling plasma at a limiter in Section 9. Corresponding arguments could also be readily applied to the cases of pellet injection and to RF-heating.

## 2. Injected Neutral Beam

Some gross effects of neutral beam injection on tokamak plasmas have been addressed in a formal way before [e.g. 1,2], often without justifying the basic assumptions of symmetry etc. Analyses based on more elementary pictures do not seem to be available in the literature, although the physics is more transparent, more subtle effects appear, and numerical estimates can be obtained quickly. On the other hand, the questions of consistency and completeness may be left more open.

To illustrate the essential features let us simplify strongly the tokamak plasma geometry to a slab model as depicted in Figure 1. A beam of neutral particles (with density  $n_0$  and velocity  $v_{0x}$ ) enters the plasma from the left, propagating perpendicularly to the magnetic field pointing the upwards in z-direction. The plasma parameters such as electron density  $n_e(x)$ , temperatures  $T_e(x)$ ,  $T_i(x)$  are assumed to vary slowly with x as compared with

$$r_g = \frac{v_{0x} \cdot m_0 c}{eB_z} \quad \dots (1)$$

For simplicity we also assume hydrogenic plasma and beam particles, i.e.  $Z=1$ . In a volume element inside the plasma, particles from the neutral beam are ionised at a rate

$$R_i = n_o \cdot n_e \langle \sigma v \rangle_i, \quad \dots (2)$$

where  $\langle \sigma v \rangle_i$  should include both electron and ion collisional ionisation. The separated electron starts to gyrate with a speed corresponding to a few eV. The newly produced ion carries practically all the injection energy and moves into a relatively large orbit given by formula (1).

There is no fundamental difference if the beam is attenuated by charge exchange (cx) collisions at a rate

$$R_{cx} = n_o \cdot n_i \langle \sigma v \rangle_{cx}. \quad \dots (3)$$

The corresponding electron, then belongs to the background plasma around the collision point.

The separation of charges obviously creates an electric field oscillating with the local ion gyrofrequency. Averaged over such periods an electric dipole remains with a moment

$$p_y = -e \cdot r_g \quad \dots (4)$$

with the radius  $r_g$  taken as the average distance between the charges.

It is, of course, not necessary that the electric field is built up between the ion and the original electron. In fact, certainly for

$$r_g > \lambda_D = \left( \frac{T_e T_i}{4\pi n_e e^2 (T_e + T_i)} \right)^{1/2},$$

where  $\lambda_D$  is the Debye length, the plasma is adjusting on a plasma frequency timescale and the ion charge is shielded by other surrounding electrons; however, all adjustments must finally add up to the basic charge separation. In other words, the created field acts mainly on the background plasma until the fast particle is slowed down by collisions, i.e. for a slowing-down period which can be roughly estimated to be

$$\tau_{sd}(\text{sec}) \approx 10^{12} \frac{T_e(\text{keV})^{3/2}}{n_e(\text{cm}^{-3})} . \quad \dots (5)$$

### 3. Polarisation Model

To estimate the total electric field we might recall the elementary theory of polarisation of dielectrics. There, an applied  $\vec{E}$ -field leads to the formation of electric dipoles which give rise to a polarisation field (in the counter direction). In our case the applied field is replaced by injection of particles. It should be noted that with fixed  $\vec{v}_0$  and  $\vec{B}$  the created dipoles are all in the same direction, so that simple addition yields the total created field

$$E = 4\pi e r_g \gamma N_f$$

with

... (6)

$$N_f = (R_i + R_{cx}) \cdot \tau_{sd}$$

representing the total number of fast ions. The factor  $\gamma$  ( $\gamma < 1$ , e.g.  $\gamma = 1/2$ ) could take into account that  $r_g$  is decreasing during a period  $\tau_{sd}$ .

If one is not willing to speculate on the lifetime of the fast ions, one could be satisfied with a creation rate (which corresponds to the initial displacement current)

$$\dot{\vec{E}} = 4\pi e r_g (R_i + R_{cx}) \quad \dots (7)$$

An analogous consideration must be made for the magnetic field. Every beam particle absorption creates also a magnetic momentum connected with the gyrating fast ion:

$$\mu = \frac{e \omega_{ci}}{2\pi c} r_g^2 \pi \quad \dots (8)$$

directed opposite to the existing magnetic field (-z direction in Fig. 1). The rate of change of the  $\vec{B}$ -field is given, in general, by

$$\dot{\vec{B}} = 4\pi \vec{\mu} \dot{N}_f = 4\pi \vec{\mu} R, \quad \dots (9)$$

or for the above example by

$$\dot{B}_z = -2\pi \frac{e}{c} \omega_{ci} r_g^2 (R_i + R_{cx}), \quad \dots (10)$$

which would result in a diamagnetic field depression of the order of

$$\Delta B_z = 4\pi \mu \dot{N}_f.$$

#### 4. Momentum Balance

In another, more macroscopic, approach the rate  $\dot{\vec{E}}$  may be obtained from conservation of momentum. Referring again to Figure 1 it is obvious that with absorption of a beam particle, its mechanical momentum  $m_o \cdot v_{ox}$  is lost, i.e. the beam loses momentum at a rate

$$-\dot{M}_x = m_o v_{ox} \cdot (R_i + R_{cx}). \quad \dots (11)$$

This momentum must appear in the momentum of the electromagnetic field (in Gaussian units), i.e.

$$\frac{d}{dt} (nm\vec{v} + \frac{1}{4\pi c} (\dot{\vec{E}} \times \vec{B})) = 0. \quad \dots (12)$$

In the rate of change for the field,

$$\frac{1}{4\pi c} \left\{ \frac{d\dot{\vec{E}}}{dt} \times \vec{B} + \dot{\vec{E}} \times \frac{d\vec{B}}{dt} \right\},$$

the second term is obviously of higher order, but it might be assessed through Eq. (9).

For our special case (Fig. 1), Eq. (12) becomes

$$\dot{E}_y = \frac{4\pi(R_i + R_{cx})}{B_z} (\mu E_y + c m_o v_{ox})$$

with the solution

$$E_y = \frac{4\pi c m_o v_{ox} (R_i + R_{cx})}{B_z} \cdot t \quad \dots (13)$$

for

$$B_z \gg \tau_{sd} \cdot 4\pi \mu (R_i + R_{cx}),$$

in agreement with formula (7).

### 5. Example

For a numerical example data related to the JET experiment are chosen:  
 $B_z = 30\text{kG}$ ,  $n_e = n_{D^+} = 3 \times 10^{13} \text{cm}^{-3}$ ,  $T_e = 3\text{keV}$ , deuterium plasma and deuterium beam.

In the beams, particles with 80keV energy are injected, adding up to a power of 10MW through a port area of  $100 \times 30\text{cm}^2$ . Evaluation of these data results in (rounded figures)

$$v_{ox} = 3 \times 10^8 \text{ (cm s}^{-1}\text{)}$$

and

$$n_o = 9 \times 10^8 \text{ (cm}^{-3}\text{)}$$

(or a flux density  $\Gamma_{NB} = 2.5 \times 10^{17} \text{ cm}^{-2} \text{ s}^{-1}$ ).

The actual injection angle deviates by about  $20^\circ$  from the normal, the effect of which is (unrealistically) ignored here but reconsidered below.

The gyration frequency  $f_{ci}$  and the radius  $r_g$  (eq. (1)) are computed to

$$f_{ci} = \frac{\omega_{ci}}{2\pi} = 2,3 \cdot 10^7 \text{ s}^{-1}$$

and

$$r_g = 2 \text{ cm.}$$

With atomic cross sections from Ref. [3] the ionic collisional ionisation with  $\langle\sigma v\rangle \approx 4.5 \times 10^{-8} \text{ cm}^3\text{s}^{-1}$  is higher than ionisation by electrons ( $\langle\sigma v\rangle \approx 2 \times 10^{-8} \text{ cm}^3\text{s}^{-1}$ ). Charge exchange is the dominant process ( $\langle\sigma v\rangle_{cx} \approx 6 \times 10^{-8} \text{ cm}^3\text{s}^{-1}$ ). Thus, the sum of the collision rates,  $R$ , is

$$R = R_i + R_{cx} \approx 3.5 \times 10^{15} \text{ (cm}^{-3}\text{s}^{-1}\text{)}.$$

Inserting these numbers into formula (7) we obtain

$$\begin{aligned} \dot{E} &= 4.2 \times 10^7 \text{ esu} \\ &= 1.3 \times 10^{12} \text{ V m}^{-1} \text{ s}^{-1} \end{aligned}$$

Estimating the slowing down time  $\tau_{sd}$  (eq. (5)) to

$$\tau_{sd} = 0.15\text{s},$$

the enormous electric field strength of

$$E = 2 \times 10^{11} \text{ V/m}$$

would be created.

The diamagnetic field depression (Eq. (10)) would amount to

$$\dot{B}_z = 4,5 \cdot 10^3 \text{ G s}^{-1},$$

so that the condition for the solution (13) is not well fulfilled; this could also be seen from the result that during a period  $\tau_{sd}$  the density of fast ions would considerably exceed that of the background and thus would invalidate some of our assumptions.

In reality there exist, however, reducing effects, several of which are discussed in the following sections.

## 6. Background Plasma Response

First of all, the background plasma acts like a dielectric to an applied field with a dielectric constant

$$\epsilon = 1 + \frac{4\pi n m_i c^2}{B^2}, \quad \dots (14)$$

(in our example,  $\epsilon = 1250$  for deuterium).

The effective electric field strength as seen by particles entering the considered volume element is then

$$E^* = \frac{1}{\epsilon} E. \quad \dots (15)$$

This holds, for example, for subsequent beam particles as well as for background particles, and could produce a drift velocity

$$\vec{w}_D = \frac{c}{B^2} (\vec{E}^* \times \vec{B}) \quad \dots (16)$$

in the example of Figure 1 in x-direction.

## 7. Oblique Beam Injection Motion along $\vec{B}$

As indicated above, real injection is not exactly perpendicular to  $\vec{B}$ . Therefore, the created fast ions move out of the considered volume element with a velocity component  $v_z$ . If we assume, as for a tokamak, the existence of closed magnetic (or drift) surfaces, the fast ions will not accumulate in their birth volume element but rather fill up a volume connected with the corresponding flux surface.

For the present estimates we replace the toroidal shell by a planar (y-z-) shell with periodic boundary conditions and length  $\ell_z = 2\pi R_t \cdot q$  with

the major torus radius  $R_t$ , and the "safety factor"  $q$  as the measure of the helical field line pitch. In a tokamak this corresponds to the case of a "rational surface" where the field lines close on themselves. Thus our estimates might, for example, be directly applicable for beam deposition inside the  $q = 1$  surface.

Assuming the fast particles to spread quickly over such a shell, the quantity  $N_f$  from formula (6) onwards should be reduced by the ratio between the beam penetrated part(s)  $F_p$  and the total area of flux surface  $F_s$

$$N_f^* = N_f \cdot F_p / F_s \quad \dots (17)$$

For the above JET example this ratio is around  $5 \times 10^{-3}$  (because of double penetration).

Here we have inserted for  $R_t = 300$  cm, for the (approximately) elliptic plasma cross-section, the half axes  $a = 110$  cm,  $b = 170$  cm, and chosen a surface about half way into the plasma.

The longitudinal motion affects, in principle, also the rates  $\dot{E}$  because a continuity equation with a flux term now determines  $\dot{N}_f$ :

$$\frac{\partial N_f}{\partial t} = - \operatorname{div}(\vec{v}_O N_f) + R - R_{sd} \quad \dots (18)$$

For the purely perpendicular injection case we approximated this equation by

$$\frac{dN_f}{dt} = R - \frac{N_f}{\tau_{sd}} \quad \dots (19)$$

with the solution (for constant source  $R$  and slowing-down time  $\tau_{ds}$ )

$$N_f(t) = R \tau_{sd} \left(1 - e^{-\frac{t}{\tau_{sd}}}\right) \quad \dots (20)$$

and

$$\dot{N}_f = R e^{-\frac{t}{\tau_{sd}}}.$$

To obtain an estimate for the flux term we observe that a particle with sufficiently large  $v_{||}$  on a tokamak flux surface returns to his birth volume element after a period

$$\tau_{||} = 2\pi R_t q / v_{||}. \quad \dots (21)$$

Dividing the flux shells into a beam penetrated part ( $R \neq 0$ ) and the rest ( $R = 0$ ) we consider the boundary surfaces  $S_1$  and  $S_2$  between both regions (see Fig. 2).

The flux through these surfaces consists of

- (a) circulating particles, simply passing through the volume element;
- (b) particles on their first circulation round.

The first kind does not contribute to the divergence term in Eq. (16). For the second kind,  $n_2$ , we take  $\tau_{||} \ll \tau_{sd}$ ,  $\Delta z \ll 2\pi R_t q$  and average over  $\Delta z$  to obtain:

$$n_2 = R \cdot \tau_{||}, \quad \dots (22)$$

which leads (outside  $\Delta z$ ) to an average density gradient

$$|\nabla n| = \frac{R \cdot \tau_{||}}{2\pi q R_t}. \quad \dots (23)$$

Resolving the divergence term for constant  $v_{\parallel}$  one arrives at:

$$(i) \quad - \operatorname{div}(v_{\parallel} N_f) = v_{\parallel} \cdot R(\Delta z) \tau_{\parallel} / (2\pi q R_t) = R(\Delta z) \quad \dots (24)$$

for the volume outside  $\Delta z$  (where the local  $R$  vanishes)

because  $n_2 = 0$  at  $S_2$  during  $\tau_{\parallel}$ , and therefore

$$\dot{N}_f = R(\Delta z) - R_{sd} \quad \dots (25)$$

and

$$(ii) \quad - \operatorname{div}(v_{\parallel} N_f) = 0 \quad \dots (26)$$

for the volume  $\Delta z$  because all particles  $n_2$  leaving, say, to the left are replaced by incoming ones from the right, and therefore

$$\dot{N}_f = R(\Delta z) - R_{sd} \quad \dots (27)$$

Thus, the same equation holds for the whole surface which justifies the above formula (17).

Equation (22), by the way, allows also an estimate of the toroidal asymmetry in the distribution of fast beam ions (using (6))

$$\frac{\Delta N_f}{N_f} = \frac{\tau_{\parallel}}{\tau_{sd}} \quad \dots (28)$$

For our example, with an injection angle of  $20^\circ$ ,  $v_{\perp} = 0,94 \cdot v_0$  and  $v_{\parallel} = 0,34 \cdot v_0$ , so that

$$v_{\parallel} = 10^8 \text{ cms}^{-1}$$

and, for  $q = 2$ ,

$$\tau_{\parallel} = 4 \cdot 10^{-5} \text{ sec.}$$

The asymmetry (28) is then

$$\frac{\Delta N_F}{N_F} = 2 \cdot 10^{-4}.$$

#### 8. Summary for beam E-field

Finally, collecting all the above corrections we obtain for  $E^*$  the estimate

$$E^*(\psi) = \frac{4\pi c m_i v_o \cdot R \cdot \tau_{sd} \cdot F_p}{\epsilon \cdot B_t \cdot F_s}, \quad \dots (29)$$

which results, for our example, in the remarkable field strength of

$$E^* = 8 \cdot 10^5 \text{ V m}^{-1}.$$

The drift velocity which all plasma particles would experience in such a field is

$$v_{DX} = 3 \cdot 10^7 \text{ cm s}^{-1}.$$

In reality, most quantities ( $R$ ,  $\tau_{sd}$ ,  $\epsilon$ ,  $B_t$ ,  $F_p$ ,  $F_s$ ) in (27) are varying with the flux surface resulting in a  $E(\psi)$  profile. However, a drift velocity of such order would suggest a flattening of profiles throughout the main beam absorption region.

A more accurate evaluation with deposition profiles and plasma particle motion in proper toroidal geometry can only be done numerically and is being prepared for a subsequent report. Here also the Pfirsch-Schlüter [4] neutralising currents for more general q-values are discussed.

It is instructive to add some energy comparisons. In the electric field the energy density

$$E_{el} = \frac{1}{8\pi} \epsilon E^2 \approx 3.5 \times 10^4 \text{ erg cm}^{-3}$$

is stored, as compared to the kinetic energy density of the fast particles of

$$E_{kin} = \frac{m_D}{2} N_F^* \cdot v_{ox}^2 = 3.4 \times 10^5 \text{ erg cm}^{-3},$$

and the background thermal energy density of

$$E_{th} = 3 \cdot nkT \approx 4.3 \times 10^5 \text{ erg cm}^{-3}.$$

The energy  $E_{el}$  must be provided out of  $E_{fast}$ ; obviously it would lead only to a minor reduction in  $v_{ox}$  ( $\approx 10\%$ ) and a corresponding correction has been neglected here in view of, for example, the choice of  $\gamma = 1$  in formula (6). However,  $E_{kin}$  is rather close to  $E_{th}$ .

#### 9. Recycling Boundary Plasma

Many of the above deliberations can be applied to plasma recycling. As indicated in Fig. 3, the plasma streams predominantly parallel to B, onto the limiter, is neutralised there, and the neutrals are said to be back-scattered into the plasma volume roughly with a cosine angular distribution around the limiter surface normal.

The incoming neutrals assume, through various atomic processes, velocities corresponding to a few, say 3, electrons volts; the density, however, must in steady state be comparable to that of the plasma in order to match the outflow.

As for the injected beam, the recycled neutral atoms are ionised or undergo charge exchange and their (perpendicular to  $\vec{B}$ ) momentum is transferred.

For a typical tokamak boundary plasma:

$$n_e = n_{D^+} = 10^{13} \text{ cm}^{-3}, T_e = T_i = 100\text{eV}$$

$$n_o = 5 \cdot 10^{12} \text{ cm}^{-3}, T_o = 3\text{eV}, B = 3 \cdot 10^4 \text{ G},$$

with  $v_{ox} = 2 \cdot 10^6 \text{ cm s}^{-1}$

we estimate the produced electric field strength with formulas directly corresponding to the ones developed for the beam case.

The slowing-down time (Eq. (5)) must be replaced here by the collision time between ions

$$\tau_i(\text{s}) = 2,1 \cdot 10^7 \cdot T_i(\text{eV})^{3/2} \left(\frac{m_i}{m_H}\right)^{1/2} / (n(\text{cm}^{-3}) \ln \Lambda),$$

which results for the above values in

$$\tau_i = 2 \times 10^{-4} \text{ s.}$$

The particle source R is estimated to be  $R \approx 4 \cdot 10^{18} \text{ cm}^{-3} \text{ s}^{-1}$ , and the dielectric constant has dropped to  $\epsilon = 430$ . The momentum balance (Eq. (13)) then yields

$$\vec{E}_y \approx 3,4 \cdot 10^8 \text{ esu,}$$

and

$$E = 2 \times 10^9 \text{ V/m.}$$

Corrected for background response ( $\varepsilon$ ) and the ratio between the surface of a belt limiter and the outermost magnetic flux surface, of about  $10^{-1}$  for the JET limiter case, we obtain in analogy to Eq. (29):

$$E^* = \frac{4\pi c m_i v_o R \tau_i F_{lim}}{\varepsilon B_t F_s} . \quad \dots (30)$$

Inserting numbers in this formula we obtain

$$E^* \approx 4.7 \times 10^5 \text{ Vm}^{-1}.$$

which is rather comparable to the  $E^*$ -value in Section 8.

We have assumed here again an almost homogeneous outer plasma layer. The mean free path  $v_{ox} \cdot \tau_i$ , however, indicates a more localised phenomenon, reducing  $F_s$  in (30).

Also this case will be considered in more detail in a future report for which a two-dimensional computational fluid plasma model in realistic geometry is evaluated.

#### Acknowledgements

I am very grateful for clarifying discussions on this paper with my colleagues at JET, T.E. Stringer and Z. Jankowicz, and with K. Elsässer of the Ruhr-Universität Bochum.

## References

- [1] J.D. Callen, R.J. Colchin, R.H. Fowler, D.G. McAlees, J.A. Rome, Proc. 5th IAEA Conf. on Plasma Physics and Contr. Nucl. Fusion Research, Tokyo, (1974), Vol. I, p. 645.
- [2] J.W. Connor, J.G. Cordey, Nucl. Fusion, 14, (1974), p. 185.
- [3] A.C. Riviere, Nucl. Fusion, 11, (1971), p. 363.
- [4] D. Pfirsch, A. Schlüter, Report MPI/PA/7/62.

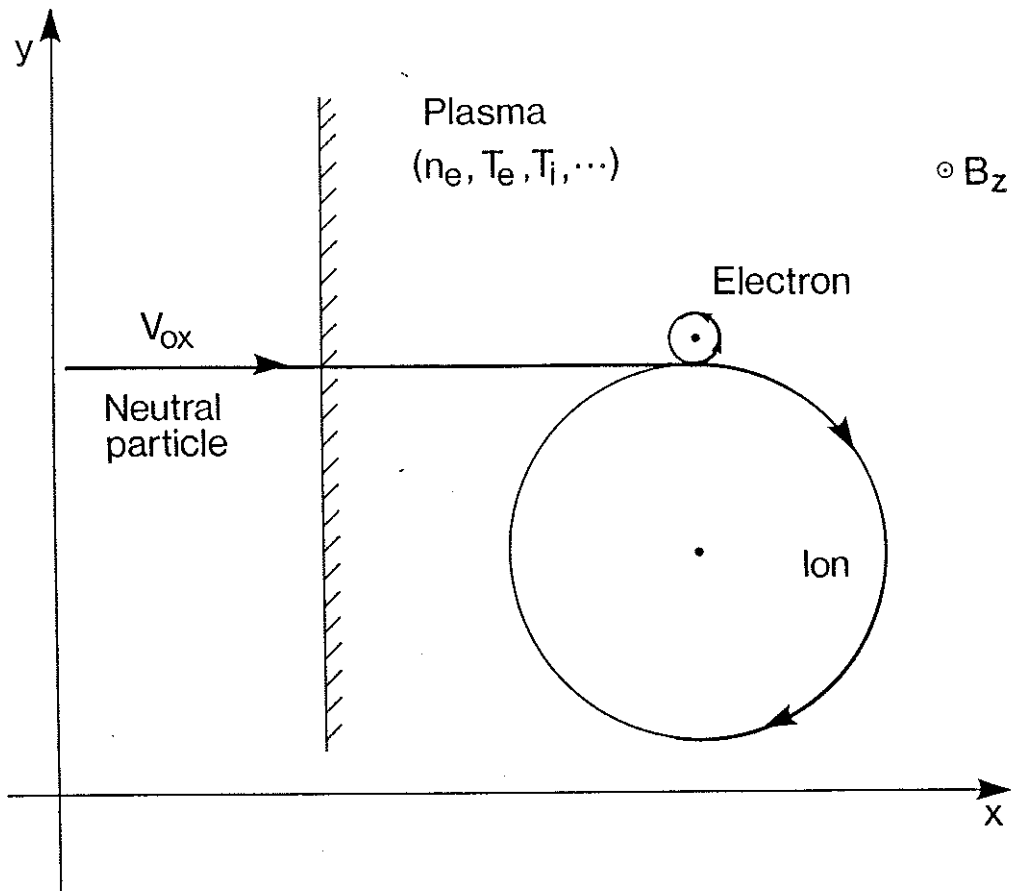


Fig. 1: Charge separation for absorbed neutral beam particle.

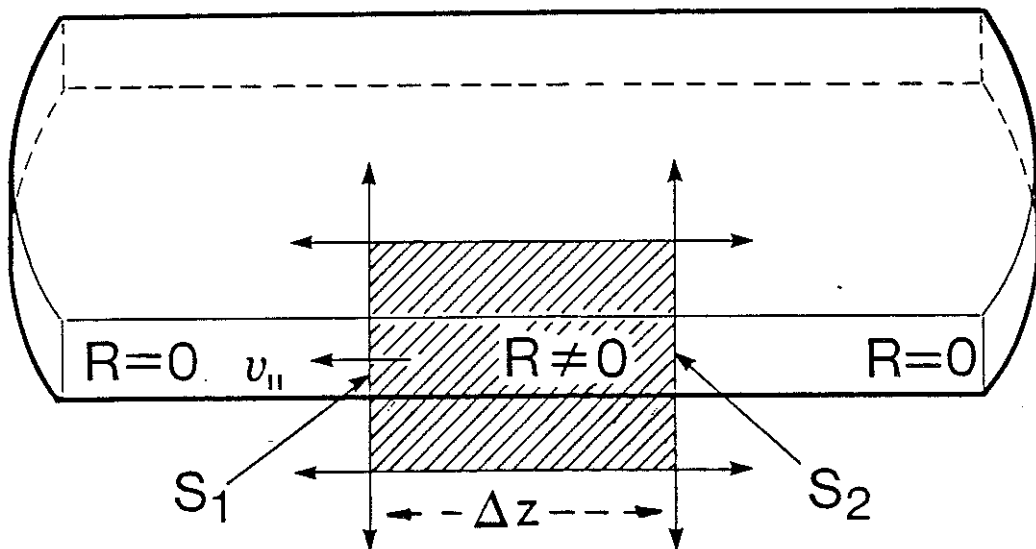


Fig. 2: Spreading of fast ions from the absorption region.

